



Research Article

Deregulation of miRNAs-cMYC circuits is a key event in refractory celiac disease type-2 lymphomagenesis

 **Valentina Vaira**^{1,*}, **Gabriella Gaudioso**^{1,2,*}, **Maria Antonella Laginestra**³, **Andrea Terrasi**¹, **Claudio Agostinelli**³, **Silvano Bosari**^{1,2},  **Antonio Di Sabatino**⁴, **Alessandro Vanoli**⁵, **Marco Paulli**⁵, **Stefano Ferrero**^{1,6}, **Leda Roncoroni**^{7,8}, **Vincenza Lombardo**⁷, **Liyanage P. Perera**⁹, **Sonia Fabris**¹⁰, **Maurizio Vecchi**^{2,7}, **Stefano Pileri**¹¹ and **Luca Elli**⁷

¹Division of Pathology, Fondazione IRCCS Ca' Granda Ospedale Maggiore Policlinico, Milan, Italy; ²Department of Pathophysiology and Transplantation, University of Milan, Milan, Italy; ³Hematopathology Unit, Department of Experimental, Diagnostic and Specialty Medicine, S. Orsola-Malpighi Hospital, University of Bologna, Bologna, Italy; ⁴Department of Internal Medicine San Matteo Hospital, University of Pavia, Pavia, Italy; ⁵Department of Molecular Medicine San Matteo Hospital, University of Pavia, Pavia, Italy; ⁶Department of Biomedical, Surgical and Dental Sciences, University of Milan, Milan, Italy; ⁷Center for the Prevention and Diagnosis of Celiac Disease, Division of Gastroenterology and Endoscopy, Fondazione IRCCS Ca' Granda Ospedale Maggiore Policlinico, Milan, Italy; ⁸Department of Biomedical, Surgical and Dental Sciences, University of Milan, Milan, Italy; ⁹Lymphoid Malignancies Branch, National Cancer Institute, Bethesda, MD 20892, U.S.A.; ¹⁰Division of Hematology, Fondazione IRCCS Ca' Granda Ospedale Maggiore Policlinico, Milan, Italy; ¹¹Division of Haematopathology, European Institute of Oncology, Milan, Italy

Correspondence: Valentina Vaira (valentina.vaira@unimi.it) or Luca Elli (luca.elli@policlinico.mi.it)

A percentage of celiac disease (CD) patients develop refractory type-2 disease (RCD2), a condition associated with increased risk of enteropathy-associated T-cell-lymphoma (EATL) and without therapeutic option. Therefore, we profiled the miRNome in series of peripheral T-cell lymphomas (PTCLs), CD, RCD1 or 2 and in the murine interleukin-15 (IL15)-transgenic (TG) model of RCD. The transcriptome was analyzed in 18 intestinal T-cell lymphomas (ITLs). Bioinformatics pipelines provided significant microRNA (miRNA) lists and predicted targets that were confirmed in a second set of patients.

Our data show that ITLs have a unique miRNA profile with respect to other PTCLs. The c-MYC regulated miR-17/92 cluster distinguishes monomorphic epitheliotropic ITL (MEITL) from EATL and prognosticates EATL outcome. These miRNAs are decreased in IL15-TG mice upon Janus kinase (JAK) inhibition. The random forest algorithm identified a signature of 38 classifier miRNAs, among which, the miR-200 and miR-192/215 families were progressively lost in RCD2 and ITL-CD, whereas miR-17/92 and C19MC miRNAs were up-regulated. Accordingly, SMAD3, MDM2, c-Myc and activated-STAT3 were increased in RCD2 and EATL tissues while JAK inhibition in IL15-TG mice restored their levels to baseline.

Our data suggest that miRNAs circuit supports activation of STAT3 and c-Myc oncogenic signaling in RCD2, thus contributing to lymphomagenesis. This novel understanding might pave the way to personalized medicine approaches for RCD and EATL.

Introduction

Celiac disease (CD) represents the most common autoimmune enteropathy in Western countries with a prevalence of approximately 1:100 individuals. The only available therapy is the gluten-free diet (GFD) that usually resolves symptoms and reverts duodenal damage. However, a minority of CD patients (approximately 5%) can develop severe and life-threatening complications such as refractory CD (RCD) and enteropathy-associated T-cell lymphoma (EATL) [1].

Refractory celiac sprue is defined by persistent malabsorptive symptoms and villous atrophy despite strict adherence to a GFD for at least 12 months. There are two types of RCD, with type 2 being more aggressive. Type 1 RCD (RCD1) shows a normal intraepithelial lymphocyte phenotype with surface expression of CD3 and CD8 markers and a polyclonal T-cell receptor (TCR) repertoire. Conversely,

*These authors contributed equally to this work.

Received: 10 January 2020

Revised: 14 May 2020

Accepted: 15 May 2020

Accepted Manuscript online:

18 May 2020

Version of Record published:

22 May 2020

RCD2 is characterized by the presence of an aberrant intraepithelial T-cell clone (IEL), which lacks surface CD3 expression but shows intracytoplasmic CD3 expression. Moreover, aberrant IELs frequently show TCR clonality [2,3]. The majority of patients with RCD2 (>60%) develop intestinal lymphoma within 5 years from the initial diagnosis, and this condition is now considered a malignant precursor of EATL [1,3]. Both RCD2 and EATL have a dismal prognosis with a mortality rate of approximately 80%. Moreover, the role of surgery as a curative strategy is limited due to complications such as perforation and multifocal nature of the diseases. Despite the known contribution of the individual's genetic background, i.e. the expression of HLA-DQ2 or HLA-DQ8 molecules as an important susceptibility factor for CD, the pathogenetics of CD and related complications are poorly understood. To date, the surveillance of RCD patients is performed using highly invasive and poorly reproducible techniques, such as capsule endoscopy or device-assisted enteroscopy with or without duodenal mucosal biopsy [3]. Finally, while TCR γ clonality and flow-cytometric evidence of the aberrant T-cell clones being diagnostic hallmarks for RCD2, [1] these are not useful biomarkers for patients' prognostication, follow-up or therapy decision-making. A pathogenic role for interleukin-15 (IL15) has been established in CD and IL15 up-regulation in the duodenal mucosa of CD subjects is now considered a feature of active disease [4]. IL15 influences every phase of CD, from the initial loss of oral tolerance to gluten, to loss of immune cell homeostasis and epithelial cell killing, eventually sustaining the expansion of the aberrant intraepithelial T lymphocytes in RCD2 disease. IL15 effects are pivotally dependent on the family of Janus kinases (JAKs). It has been shown that JAK inhibition through Tofacitinib, a pan-JAK inhibitor (JAKi), reverts the intestinal damage in the transgenic (TG) mouse model that overexpresses IL15 specifically in the enterocytes (T3^b-hIL-15 Tg mice) [5,6]. We have previously characterized the microRNA (miRNA) profiles in different CD phenotypes, highlighting that the miR-192/215 family is down-regulated in patients with active CD in spite of GFD [7].

In the present study, extending our previous observation, we have profiled the miRNome in the IL15 TG mice treated or not with the pan-JAKi Tofacitinib and in a series of intestinal T-cell lymphomas (ITLs), RCD and CD to gain compelling evidence of miRNA dysregulation during lymphomagenesis of aberrant IELs. Moreover, we aimed to identify molecular signatures with prognostic relevance that may support clinicians in designing a personalized medicine approach for RCD patients.

Materials and methods

Peripheral T-cell lymphoma samples

A series consisting of 21 peripheral T-cell lymphoma (PTCL) not otherwise specified (PTCL-NOS), six ALK-positive and four ALK-negative anaplastic large cell lymphomas (ALCLs), ten angioimmunoblastic T-cell lymphoma (AITL) have been previously described [8] and total RNA was available for this study.

Intestinal lymphoma samples

A series of 23 ITLs was retrieved from the archives of Sant'Orsola Hospital (Bologna, Italy) and immunophenotyped according to current WHO guidelines [9]. Briefly, the antibody panel included CD2, CD3, CD4, CD5, CD7, CD8, CD20, CD30, CD56, CD103, β F1, TIA1, Perforin, Granzyme B and KI67. Moreover, TCR clonality and Epstein–Barr virus (EBV) presence were assessed and recorded as well. According to this panel, ITL were categorized as EATL ($n=14$), monomorphic epitheliotropic ITL (MEITL; $n=7$) or EBV-positive extranodal nasal-type NK/T-cell lymphoma (EBV^{pos}-ENKL; $n=2$). This latter type of lymphoma was excluded from the analysis of intestinal lymphoma samples. Among EATL or MEITL, 12 (86%) and 1 (14%) patients had history of CD. For 18 patients, survival data were available. Samples characteristic are detailed in Table 1. A second cohort of seven EATL originated in celiac patients (from Fondazione IRCCS Ca' Granda Hospital) was used for target expression analysis (Supplementary Table S1).

CD samples

Duodenal biopsies from an initial set of patients with CD at first diagnosis ($n=5$; CD), patients with CD under GFD with ($n=5$; CD in remission, r-CD) or without ($n=5$; active CD, a-CD) normalization of villous atrophy, refractory type 1 CD ($n=4$; RCD1) or with refractory type 2 CD ($n=5$; RCD2) were retrieved from the archives of the Division of Pathology of Fondazione IRCCS Ca' Granda (Milan, Italy) or IRCCS San Matteo (Pavia, Italy) hospitals and used for miRNA profiling. Patients' characteristics are detailed in Table 2. A second set of five RCD1, ten RCD2 from Fondazione IRCCS Ca' Granda Hospital was used for target expression analysis by immunohistochemistry (IHC, Supplementary Table S1). RCD was diagnosed according to the Oslo definition [10] and recent updates [11]. Briefly, CD patients who showed absence of clinical remission after 1 year of a correct GFD verified by an expert nutritionist and the maintenance of villous atrophy at histology suggested the presence of a refractory state. RCD2

Table 1 Clinicopathological characteristics of the intestinal lymphomas studied for miRNA profiling

Clinical features						Immunohistochemistry ¹													Molecular features ²			
ID	Gender	Subtype	CD	Status ³	OS months	CD2	CD3	CD4	CD5	CD7	CD8	CD20	CD30	CD56	CD103	β F1	TIA1	Granzyme			EBV	TCRγ
																		B	Perforin	KI67		
ITL1	F	EATL	yes	1	12	0	1	0	0	1	1	0	0	0	0	0	1	1	1	1	0	1
ITL2	M	MEITL	no	1	2.5	1	1	0	1	1	1	na	na	na	na	na	na	na	na	0	na	na
ITL4	M	EATL	yes	1	10	0	1	1	0	1	0	0	1	na	na	na	na	1	na	1	na	na
ITL5	F	MEITL	no	na		1	1	0	0	1	1	0	0	1	0	1	1	na	na	na	0	0
ITL6	F	EATL	yes	1	4	0	1	0	0	1	1	0	1	0	1	0	1	0	1	1	0	0
ITL7	M	EATL	yes	1	2	na	1	na	na	na	na	0	1	0	na	1		na	1	1	0	0
ITL8	M	MEITL	yes	1	1	1	1	0	1	1	1	0	0	1	1	0	1	0	1	1	0	1
ITL10	F	MEITL	no	1	6	1	1	0	0	1	1	0	0	1	0	1	1	0	1	1	0	1
ITL11	F	EATL	yes	1	7	1	1	1	0	1	0	0	1	0	1	0	1	1	1	1	0	0
ITL27	F	EATL	yes	0	60	0	1	0	0	1	0	0	1	0	0	0	1	1	1	1	0	na
ITL30	M	EATL	no	1	5	1	1	1	0	1	0	0	1	0	0		1	1	1	0	0	0
ITL35	M	EATL	yes	0	60	0	0	0	0	1	0	0	1	0	1	0	1	1	0	1	0	0
ITL37	F	EATL	yes	1	2	0	1	0	0	1	0	0	1	0	1	0	1	1	1	1	0	1
ITL39	M	EATL	yes	1	18	0	1	1	na	1	0	na	1	0	na	0	1	na	1	1	na	0
ITL41	M	EATL	yes	1	25	1	1	0	0	1	0	0	0	0	1	1	1	1	1	0	0	0
ITL45	F	MEITL	no	0	24	0	1	0	0	1	1	0	0	0	1	0	1	na	1	1	0	1
ITL47	M	MEITL	no	1	12	0	1	0	0	1	1	0	0	1	1	0	1	1	1	1	0	na
ITL53	F	EATL	yes	0	22	1	1	1	0	1	0	0	1	0	1	0	1	1	1	1	0	0
ITL56	M	MEITL	no	na		na	1	na	na	na	na	0	na	1	na	na	na	na	na	1	na	na
ITL57	F	EATL	no	na		0	1	0	0	1	1	0	1	0	na	0	1	1	1	1	na	0
ITL60	M	EATL	yes	na		1	1	1	1	1	0	na	1	0	na	na	1	na	1	1	na	na

¹0, absent; 1, present; na, information not available; for KI67 staining, ITL with a percentage of positive cells below 50% were considered 0.

²EBV, Epstein–Barr virus; TCRγ, clonality of T-cell receptor γ; 0, absent; 1, present; na, information not available.

³0, censored; 1, deceased.

Table 2 Clinicopathological characteristics of the CD patients studied for miRNA profiling

ID	Gender	Subtype ¹	Classification ²	TCR-clonality ³	Evolution to EATL	Status
CD11	F	Active	3b	na	No	Alive
CD12	F	Active	3a	Polyclonal	No	Alive
CD13	M	Active	3a	na	No	Alive
CD14	F	Active	3a	na	No	Alive
CD15	F	Remission	na	na	No	Alive
CD16	F	Remission	0	na	No	Alive
CD17	F	Remission	1	na	No	Alive
CD18	M	Remission	0	na	No	Alive
CD19	F	Remission	2	na	No	Alive
CD20	F	At diagnosis	3a	na	No	Alive
CD21	F	At diagnosis	3a	na	No	Alive
CD22	F	At diagnosis	3c	na	No	Alive
CD23	F	At diagnosis	3c	na	No	Alive
CD24	F	At diagnosis	3a	na	No	Alive
RCD17	F	RCD1	3b	na	No	Deceased
RCD18	F	RCD1	3c	na	No	Alive
RCD19	F	RCD1	3c	na	No	Alive
RCD20	M	RCD1	3a	na	No	Alive
RCD12	F	RCD2	3b	Monoclonal	No	Alive
RCD13	F	RCD2	3a	na	No	Alive
RCD14	F	RCD2	3c	Monoclonal	No	Alive
RCD15	M	RCD2	3c	Monoclonal	Yes	Deceased
RCD16	M	RCD2	3c	Monoclonal	Yes	Deceased

¹Active, presence of villous atrophy in spite of GFD; remission, absence of villous atrophy after GFD; At diagnosis, newly diagnosed CD patient; RCD1, refractory type 1 CD; RCD2, refractory type 2 CD.

²According to Marsh–Oberhuber criteria.

³TCR; na, not available information.

diagnosis was made if the following two criteria were present: (i) the presence at flow cytometry of a relevant (>20%) quote of duodenal intraepithelial lymphocytes (IEL) with the aberrant phenotype (positive for intracytoplasmic CD3 and negative for surface CD3) and (ii) mono/oligoclonality for TCR γ . Conversely, the absence of these two markers identified RCD1 condition.

The present study was carried out in accordance with the World Medical Association Declaration of Helsinki and approved by the local Ethic Committee (IRB#278_2015). All subjects provided written informed consent.

Preclinical model of RCD

The TG mice that express human IL-15 specifically in enterocytes (T3b-hIL-15 Tg mice) have been previously described [5,6]. Aged-matched non-TG littermates (WT) were used as control for baseline miRNA expression (calibrator). Animal experiments were previously approved by the Institutional Animal Care and Use Committee [6]. Briefly, animals at 11 and 13 weeks of age ($n=4$ mice per condition) were used. Formalin-fixed paraffin-embedded (FFPE) blocks with small intestinal mucosa from wild-type (WT), TG or TG treated with the pan-JAKi Tofacitinib were used for miRNA profiling. miRNA data in TG or JAKi mice were expressed as differences with respect to the calibrator (\log_2 -transformed values).

RNA purification

Separation of lymphomatous from enterocyte component was achieved by laser-assisted microdissection (LMD6000; Leica Microsystems) as described [12]. Then, total RNA was purified from all human or murine samples using the MasterPure RNA Purification Kit (Epicentre, an Illumina company) followed by genomic DNA digestion with RNase-Free DNase I (Epicentre) as previously described [7].

Gene and miRNA expression analysis

The transcriptome of 18 ITL cases (12 EATL and 6 MEITL) was analyzed using the cDNA-mediated Annealing Selection extension and Ligation (DASL) platform (Illumina) and 500 ng of DNA-free total RNA as described [8]. Then, raw data were quantile-normalized and log₂-transformed using the lumi package within Bioconductor environment [13].

For miRNA profiling, 200 ng of DNA-free total RNA were reverse transcribed and pre-amplified using human or rodent Megaplex Primers Pools A and B (Thermo Fisher Scientific). miRNA quantification was obtained using the Taqman TLDA cards A and B as described [12]. Only miRNAs with raw mean value minus one standard deviation having <35Ct passed the filter and were included in the analyses. miRNA relative quantification (RQ) was achieved using the global mean method followed by log₂ transformation for normalization. When individual miRNAs were analyzed, total RNA was reverse transcribed with specific primers and TaqMan assays were used for qPCR. In this case, the mammary U6 ncRNA was used as reference transcript.

IHC

The presence of c-MYC (clone Y69, Dako, Agilent Technologies Inc.), phosphorylated-STAT3 at Tyr⁷⁰⁵ (clone D3A7, Cell Signaling Technologies), SMAD3 (clone 2C12, Sigma–Aldrich), and MDM2 (clone IF2, Merck KGaA), was analyzed in human tissue sections by IHC using the Dako Omnis or the Ventana Benchmark Ultra autostainer as described [14]. Immunoreactivity was revealed using DAB as chromogen or the Ultraview Red Detection Kit and staining of the lymphocytic infiltrate was separately scored as percentage of positive cells. When mice tissues were processed for IHC, the Rodent block M reagent (BioCare Medical, Pacheco, CA, U.S.A.) was added to the slides prior to primary antibody as suggested by the manufacturer.

Fluorescence *in situ* hybridization

The genetic status of c-MYC was analyzed in three RCD2 and five EATL samples from the validation series using fluorescence *in situ* hybridization (FISH) technique. Briefly, FFPE tissues underwent digestion using the Poseidon kit (Leica Microsystems, Milan, Italy) and then were hybridized with an LSI-MYC dual color, break apart rearrangement probe (Abbott Laboratories, Abbott Park, IL, U.S.A.) following manufacturer's protocol. DAPI was used to counterstain nuclei. As positive control for c-MYC amplification we used a radiotherapy-associated angiosarcoma (RAS) of the breast.

Data analysis

Gene or miRNA expression data were analyzed by both unsupervised and supervised test. Briefly, the ComplexHeatmap package available in Bioconductor was used for hierarchical clustering analysis, and *K*-means clustering algorithm was used to visualize set of co-regulated miRNAs. Principal component analysis (PCA; <https://cran.r-project.org>) was used to visualize patients' distribution according to the miRNome or selected miRNAs as described [15]. Pearson analysis (R studio) was used to assess samples similarity using the Silhouette method. The non-negative matrix factorization analysis (NMF) from Genepattern (<https://cloud.genepattern.org/>) was used for unsupervised samples clustering. Lists of significant miRNAs were obtained using the Kolmogorov–Smirnov test and computing the fold-change (Log₂Ratio, L2R). All *P*-values were corrected for multiple comparisons using the false discovery rate (FDR) approach. To identify 'classifier' miRNAs, we used the decision tree-based classification method RandomForest available within R environment [16].

Receiver Operating Characteristic (ROC) curve and the Youden's J statistic was used to identify cutoffs in CD56 gene expression to sort ITL cases into positive or negative group when immunohistochemical evaluation of the protein was missing. Correlation of molecular variables with patients' survival was performed using Log-Rank test (MedCalc software). Differences among samples' groups were performed using Mann–Whitney U or Kruskal–Wallis test as appropriate.

miRNAs' targets were searched using the miRTargetLink Human tool (<https://ccb-web.cs.uni-saarland.de/mirtargetlink/>), which provides list of experimentally validated miRNA targets and only genes predicted to be targeted by the miRNA with 'strong evidence' were used for Gene Ontology and pathways analysis using STRING (<https://string-db.org/>) [17].

All statistics were two-sided and *P*-values less than 0.05 were considered statistically significant unless otherwise indicated.

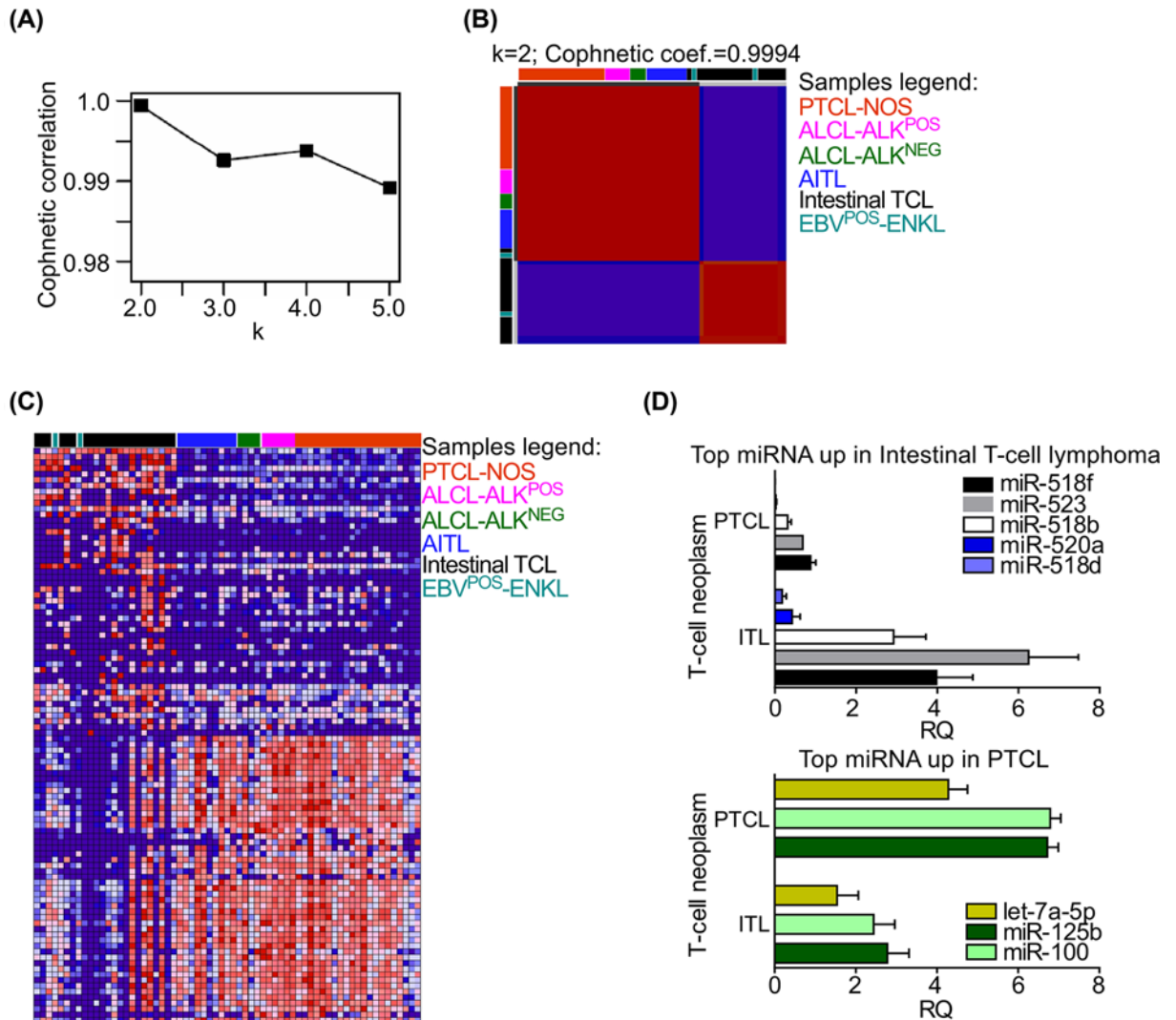


Figure 1. ITLs carry a distinctive miRNA signature in comparison with other PTCLs

(A,B) The miRNome was analyzed in different PTCL subtypes. Unsupervised NMF analysis sorted the samples into two main groups (a), and all ITLs but one case were classified in the same cluster (b). (C) Heatmap of the top 50 miRNAs mostly expressed by ITLs or by other PTCLs. Blue, low expression; Red, high expression. (D) Among the top miRNAs over-represented in ITL or other PTCLs were respectively members of the C19MC cluster (namely miR-518f, miR-523 and miR-518b; top panel) or the lncRNA MIR100HG-derived miRNA miR-100, and miR-125b (lower panel). Bars, mean \pm standard error of the mean (SEM). TCL, T-cell lymphoma.

Patient and public involvement statement

Patients and public were not involved in any phase of the research because of its retrospective nature. Indeed, all experiments were performed on archival FFPE tissue blocks.

Results

ITLs are characterized by a unique miRNA profile with respect to other types of PTCLs

We started our study looking at the global expression of miRNAs in different types of T-cell lymphomas, such as PTCL-NOS, ALK-positive or negative anaplastic large cell lymphoma, AITL, EBV positive (EBV^{POS}) extranodal NK/T-cell lymphoma and ITLs. By unsupervised NMF analysis, ITL showed a distinct miRNA profile in comparison with other PTCLs (Figure 1A,B). Interestingly, the two EBV^{POS}-extranodal NK/T-cell lymphomas originated in

the bowel also clustered together with ITLs. Looking at top miRNAs specifically enriched in ITLs or in the other subtypes of PTCL (Figure 1C; Supplementary Table S2), we identified that the C19MC miRNA cluster was expressed more in intestinal lymphomas whereas the miRNAs transcribed from the MIR100HG lncRNA, namely miR-100, let-7a-5p and miR-125b, were over-represented in PTCLs (FDR-adjusted P -value <0.05 ; Figure 1D).

c-Myc regulated miRNAs distinguish MEITL from EATL and are markers of poor prognosis in EATL patients

Next, we interrogated the miRNome of ITL in depth. Based on the new WHO classification we sorted cases into EATL or MEITL on the basis of on their morphology, immunophenotype and Ki67 index (Table 1) or CD56 expression at mRNA level if IHC was unavailable (Supplementary Figure S1A). The two EBV^{POS}-extranodal NK/T-cell lymphoma cases were excluded from the analysis. At unsupervised level the miRNome was unable to distinguish EITL from MEITL cases (Figure 2A). We therefore searched for differentially expressed miRNAs between the two histotypes, and 29 miRNAs were identified (Supplementary Table S3 and Supplementary Figure S1B). Performing hierarchical clustering of all samples with significant miRNAs, we observed that all MEITL but one grouped under a specific cluster, whereas EATL showed a high degree of intertumor heterogeneity and clustered into three different branches, designated as clusters A, B and C (Figure 2B). This organization of EATL in three principal subclusters was also conserved when we reconsidered samples distribution using the totality of microRNAs in an unsupervised analysis (Supplementary Figure S1C). Among the significant miRNAs, 6 belonged to the c-Myc up-regulated miR-17/92 and its paralogs miR-106a/363 and miR-106b/25 miRNA clusters, namely miR-20b-5p, -19b-3p, -17-5p, -106a-5p, -92a-3p and miR-19b-1-5p (Figure 1B) [18]. Besides being up-regulated in MEITL as compared with EATL, these miRNAs showed differential expression within EATL grouped into the three subsets, with cluster-C EATL showing miRNAs levels comparable with MEITL (Figure 2C). We then analyzed the expression of known c-Myc associated transcripts [5] in MEITL and EATL grouped into the three subclusters (Supplementary Table S4). In agreement with miRNA data, unsupervised analysis of c-Myc related transcripts distinguished EATL in clusters A and B from EATL in cluster C, which grouped with MEITL ($P=0.02$ by Fisher's exact test; Figure 2D). Specifically, the c-Myc activated transcripts ENO1, RPL11, STAT3 and SMAD4 were expressed more in cluster C-EATL and MEITL than in EATL from subclusters A or B ($P<0.05$ by Kruskal–Wallis test; Figure 2E). The activation of c-Myc signaling in cancer is usually associated with poorer prognosis. Therefore we analyzed survival curves of EATL sorted into the three subsets. As expected, patients belonging to cluster C had the worst prognosis (HR cluster C = 7.2; $P=0.06$; Figure 2F), recapping the outcome of MEITL patients (Supplementary Figure S1D,E). Finally, we took advantage of a preclinical model of EATL/RCD, i.e. the TG mice that express human IL-15 in enterocytes (T3^b-hIL-15 Tg mice) [5,6] in order to analyze c-Myc regulated miRNAs in the duodenum of animals treated (JAKi; Figure 2G) or not (TG; Figure 2G) with the pan-JAKi, Tofacitinib. Thirteen out of 18 miRNAs belonging to the miR-17 family were expressed in all mice (72%). With the exception of miR-106b-3p and miR-93-3p, all the miRNA belonging to the miR-17 family were decreased after the treatment (Figure 2G). This result, together with the observation that miR-17/92 miRNAs are overexpressed in EATL with worse outcome, supports a role for the miR-17 family of miRNAs in EATL pathogenesis.

Random forest analysis identifies a signature of 38 miRNAs that defines CD-associated ITL, RCD2 or RCD1 and classic CD

We then sought to investigate whether duodenal samples from patients with RCD, had a global miRNAs profile similar to intestinal lymphomas, to PTCLs, or were unrelated to both neoplastic conditions. By unsupervised analysis, RCD1 and RCD2 samples grouped together with intestinal lymphomas in two clusters separately from PTCL-NOS, ALK-positive or negative anaplastic large cell lymphoma and AITL (Figure 3A). We then focused on patients with previous or current history of CD and we analyzed if miRNAs were able to discriminate intestinal lymphomas from RCD2, RCD1 or from less aggressive forms of CD (Tables 1 and 2). PCA showed that, globally, miRNAs discriminated CD patients with intestinal lymphoma, or with RCD2, whereas patients with RCD1 were grouped with CD subjects with less severe disease (Figure 3B). Therefore, we searched for miRNA signatures specific to the different classes of disease using the Random Forest algorithm either separating (Figure 3C) or not (Figure 3D) RCD1 from CD. Confirming what was observed at unsupervised analysis (Figure 3B), RCD1 could not be distinguished from CD (Figure 3C; misclassification rate for RCD1 = 100%). Conversely, when RCD1 and CD were grouped in a single class (CD_RCD1) all cases were correctly classified by the algorithm, as well as 4 out 5 RCD2 and 12 out of 13 intestinal lymphomas (ITL-CD) (overall misclassification rate of 5.4%; Figure 3D). Top discriminating miRNAs were then identified based on the MeanDecreaseGini (≥ 0.118) and P -value (<0.05 ; Figure 3E). According to these criteria, 38 miRNAs were included in the classifier (Supplementary Table S5). When a similarity analysis between samples

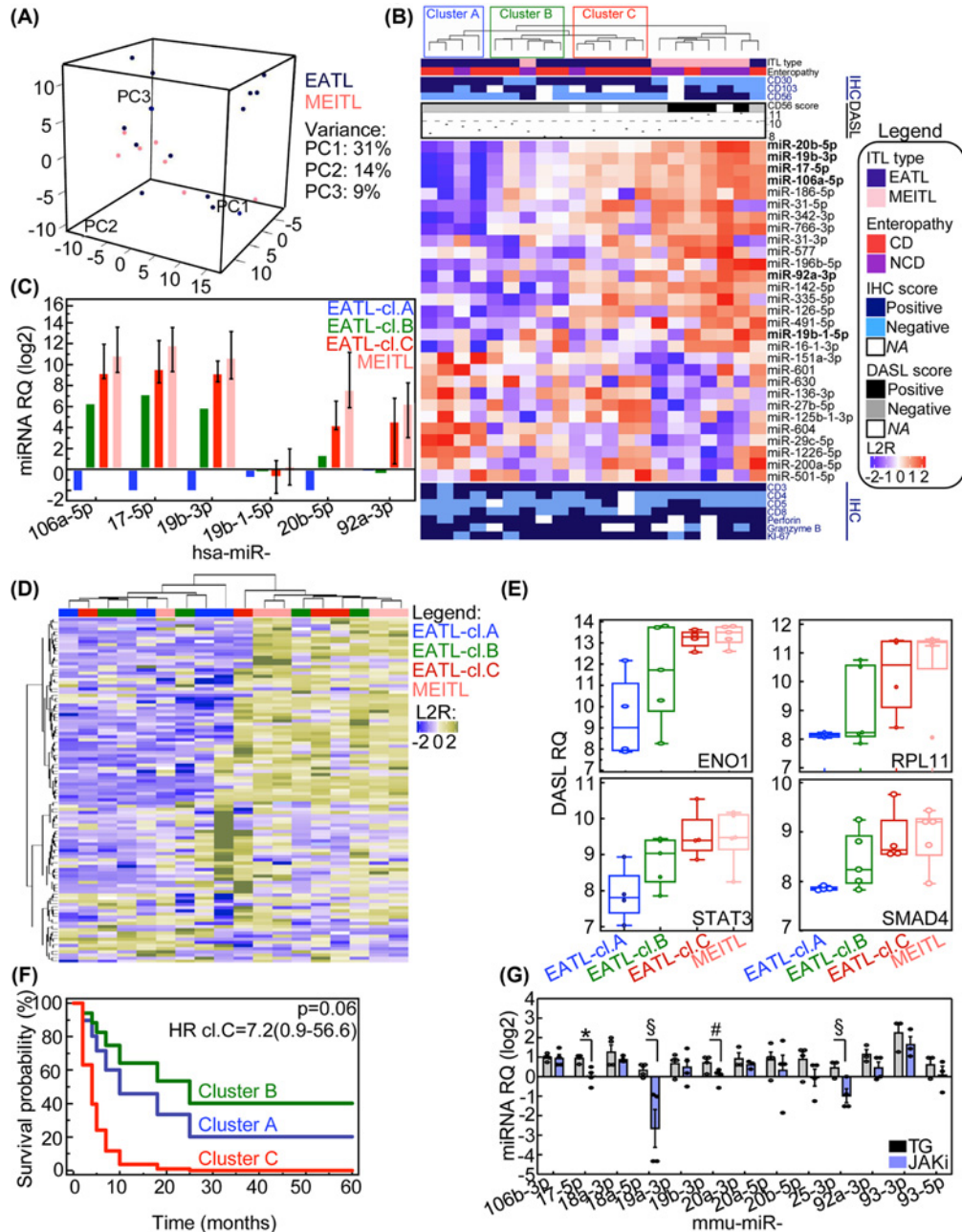


Figure 2. miR-17/92 and paralogues are overexpressed in MEITL and identify EATL with worse prognosis

(A) PCA shows that the miRNome does not distinguish EATL from MEITL at unsupervised level. (B) Heatmap of significantly different miRNAs in EATL and MEITL samples. When CD56 immunophenotype could not be detected by IHC, gene expression data (DASL) were used for ITL classification. miRNA in bold are from the miR-17/92 cluster or paralogues. (C) The indicated miRNAs were analyzed in the three EATL subgroups (identified in panel B) and in MEITL specimens. Bars, mean \pm SD. (D,E) Transcripts known to take part in c-MYC signaling were analyzed in EATL and MEITL. Unsupervised samples clustering (D) shows that, as for the miR-17/92, cluster C-EATL and MEITL share similar gene expression patterns, and are enriched in the same branch of the dendrogram ($P=0.02$, by Chi-square test). The expression of significantly different transcripts among EATL subsets, shows similar genes levels in cluster C-EATL and MEITL (E). Box and whiskers represent lowest-to-highest and median values. Each dot is a sample. (F) Kaplan–Meier curves of EATL sorted into the three different classes according to miR-17/92 miRNAs levels. HR, hazard ratio, 95% CI, 95% confidence interval. CI.C, cluster C-EATL. (G) The indicated miRNAs were analyzed in T3b-hIL-15 Tg transgenic mice treated (JAKi) or not (TG) with the JAKi Tofacitinib. Aged-matched non-TG littermates were used as calibrator and data are expressed as differences in respect to the calibrator (log₂-transformed values). *, $P=0.01$; §, $P=0.03$; #, $P=0.049$ by Mann–Whitney U test. Bars represent mean \pm SEM ($n=4$) and each dot is a sample.

Downloaded from <https://portlandpress.com/clinsci/article-pdf/134/10/1151/881988/CS-2020-0032.pdf> by guest on 29 July 2020

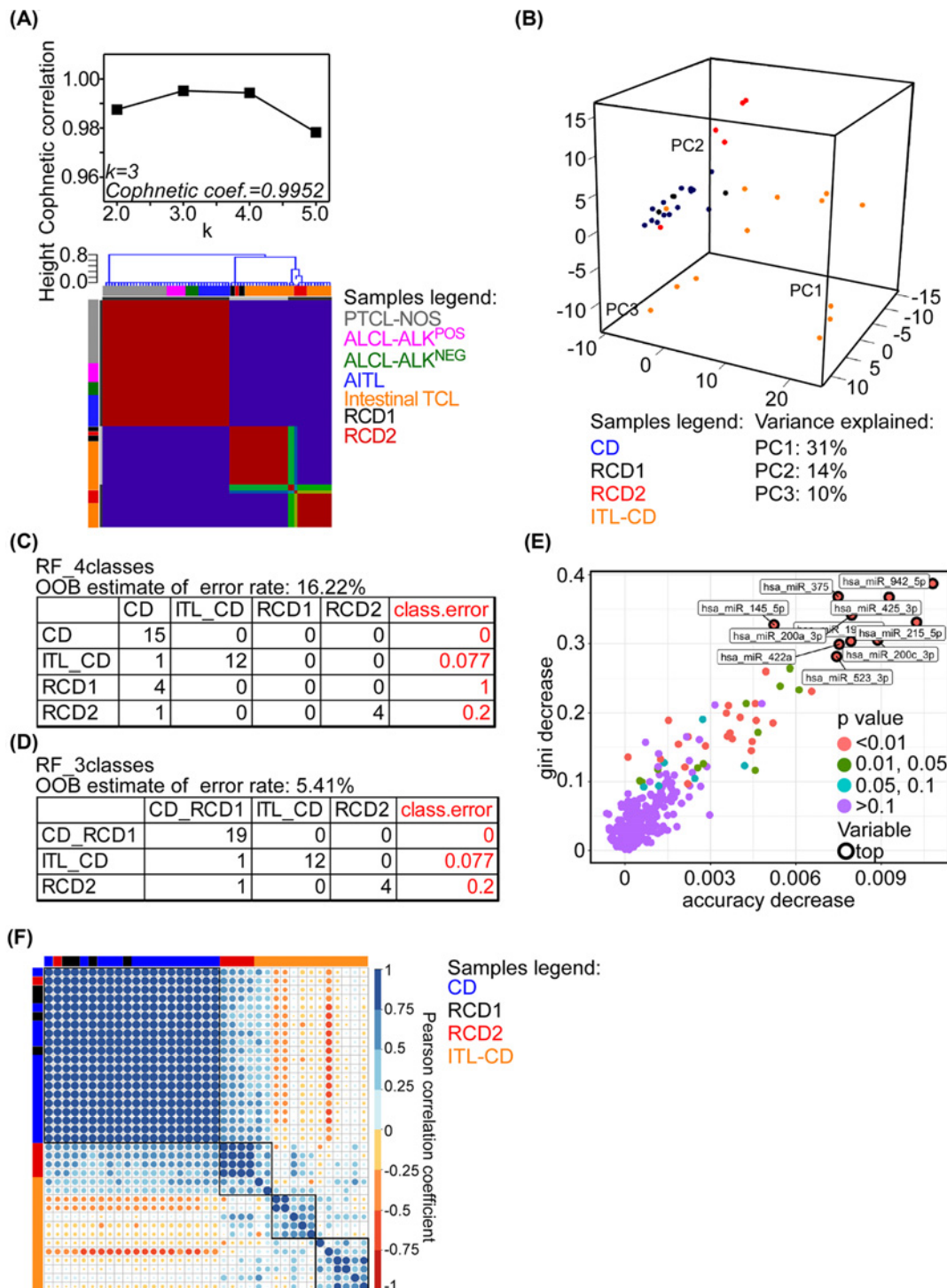


Figure 3. Identification of a miRNA signature for classifying RCD2 apart from ITL or CD patients

(A) NMF analysis was performed using the miRNome from all PTCL types, ITL, RCD1 and RCD2. RCD1 and 2 samples cluster with ITL and separately from PTCLs. (B) PCA with all miRNA was performed considering only CD patients with different diseases (CD, RCD1 or 2, ITL). PC, principal component. (C,D) The random forest (RF) algorithm was used to identify miRNAs able to sort CD patients with different diseases into separate classes. When the algorithm was asked to identify four groups of disease (ITL, RCD2, RCD1, CD), a high misclassification rate was observed (C; 16.2%). When only three classes were considered (ITL, RCD2, RCD1 with CD), the misclassification rate dropped to 5.4% (D); one case with RCD2 and one ITL were classified as CD_RCD1). OOB, out of bag. (E) RF-top 'classifier' miRNAs according to three criteria: gini decrease, accuracy decrease and *P*-value. (F) Pearson's correlation analysis was performed with the RF-miRNA signature to evaluate samples' similarity.

was performed based on the 38 miRNAs-classifier, RCD2 showed to be more similar to CD and RCD1 cases than to the majority of ITL-CD (Figure 3F). These data suggest that RCD2 is a distinct disease with a specific miRNA dysregulation profile, but still retains greater similarity to CD than to lymphoma from a molecular perspective.

The miR-200 and miR-192/215 families are progressively lost in RCD2 and intestinal lymphomas

The 38-miRNAs signature was then visualized in all samples using heatmap, and miRNAs subgrouping was performed using the *k*-means clustering algorithm. This analysis generated four miRNA subgroups in which *k*-means cluster 1 and 2 included miRNAs underexpressed in ITL-CD cases while *k*-means cluster 3 and 4 included miRNAs overexpressed in intestinal lymphomas of CD patients (Figure 4A). Interestingly, while *k*-means cluster 1 and 3 contained miRNAs specifically dysregulated only in neoplastic samples, *k*-means cluster 2 and 4 included miRNAs whose expression was similar both in ITL-CD and RCD2 cases as opposed to what was detected in RCD1 or CD patients (Figure 4A). Among the top down-regulated miRNAs in ITL-CD and in ITL-CD and RCD2 were members of the miR-200 and miR-192/215 families (9 out of 24 transcripts; Supplementary Table S5). When bioinformatics prediction of potential targets was performed (Supplementary Tables S6 and S7), cell cycle and cancers related pathways emerged as mostly affected by *k*-means cluster 1 and 2 miRNAs (Supplementary Tables S8 and S9 respectively and Supplementary Figure S2A,B) but transcriptional dysregulation in cancer, Th17 cell differentiation, p53 and TGF- β signaling were more significantly affected by cluster 2 miRNAs (Supplementary Figure S2B and Supplementary Table S9). To provide preliminary insights into dysregulation of these signaling in CD-related enteropathies, we first searched if predicted targets were inversely correlated with *k*-means cluster 2 miRNAs in our series of CD-ITL. We confirmed that SMAD3, Cdc42, and MDM2 could be targeted by at least one miRNA from *k*-means cluster 2 (Figure 4B and Supplementary Figure S3A). Next, we looked at targets protein expression in an independent set of EATL, RCD2 and RCD1 samples (Supplementary Table S1) by IHC. In line with miRNA data, we found that SMAD3 expression was progressively increased in T cells of RCD2 and EATL tissues compared with RCD1 (Figure 4C,D and Supplementary Figure S3B,C), whereas MDM2 was predominantly expressed in RCD2 compared with RCD1 or EATL (Figure 4E).

Finally, *k*-means cluster 1 and 2 miRNAs down-regulation was partially reversed in the IL15-TG mice treated with the pan-JAKi (Supplementary Figure S3D,E). In line with this, MDM2 and SMAD3 proteins expression was lower in the intestinal mucosa of mice treated with the JAKi (Supplementary Figure S3F,G). Altogether, these data point to a role for the miR-200 and miR-192/215 miRNA families in the progression of CD from refractory disease toward a neoplastic stage at least in part through the regulation of SMAD3/MDM2 signaling.

The oncomiRNAs belonging to the miRNA clusters miR-17/92 and C19MC are up-regulated in RCD2 and ITL-CD

Among the miRNAs significantly overrepresented in both lymphomatous and RCD2 samples (*k*-means cluster 4) were members of the miR-17/92 cluster (namely miR-18b-5p and miR-363-3p) and C19MC miRNA cluster (namely miR-517c-3p and miR-523-3p), two recognized families of onco-miRNAs. Among the pathways activated by miR-17/92 miRNAs is *c-Myc* [19] and a recent report also described the existence of an oncogenic circuit between C19MC and *n-MYC* in embryonal tumors with multilayered rosettes (ETMRs) [20]. Moreover, *k*-means cluster 4 miRNAs were inversely correlated with *c-Myc* mRNA in EATL (Figure 5A). Therefore, we analyzed *c-Myc* and activated Signal Transducers and Activators of Transcription 3 (STAT3 phosphorylated at Tyr⁷⁰⁵ residue) in duodenal biopsies from celiac patients with EATL, RCD2 or RCD1. While *c-Myc* was overexpressed mainly in lymphomas (Figure 5B,C), STAT3 was significantly more activated in the aberrant lymphocytic compartment of RCD2 and EATL than in RCD1 (Figure 5B,C and Supplementary Figure S4A). This observation is in line with the fact that STAT3 acts upstream of *Myc* and suggests that STAT3 activation and nuclear accumulation precedes *c-Myc* overexpression [21,22]. Accordingly, activated STAT3 was decreased upon JAK signaling inhibition in IL15-TG mice (Supplementary Figure S4B). Finally, FISH analysis of *c-MYC* status in EATL and RCD2 tissues evidenced that a fraction of EATL cells display *c-MYC* gene amplification (range 1–17%) and that this mechanism is not clonal. No RCD2 sample showed gain in *c-MYC* copies (Figure 5D and Supplementary Figure S5A–C). Finally, *c-MYC* amplification did not consistently explained protein overexpression detected in EATL, as there was no direct association between FISH and IHC quantification of positive nuclei (Figure 5E). Therefore, these data suggest that an oncogenic network between *Myc* signaling and miRNAs belonging to the C19MC and miR-17/92 clusters possibly promotes neoplastic transformation of aberrant T lymphocytes in the enteric mucosa of RCD patients (Figure 6).

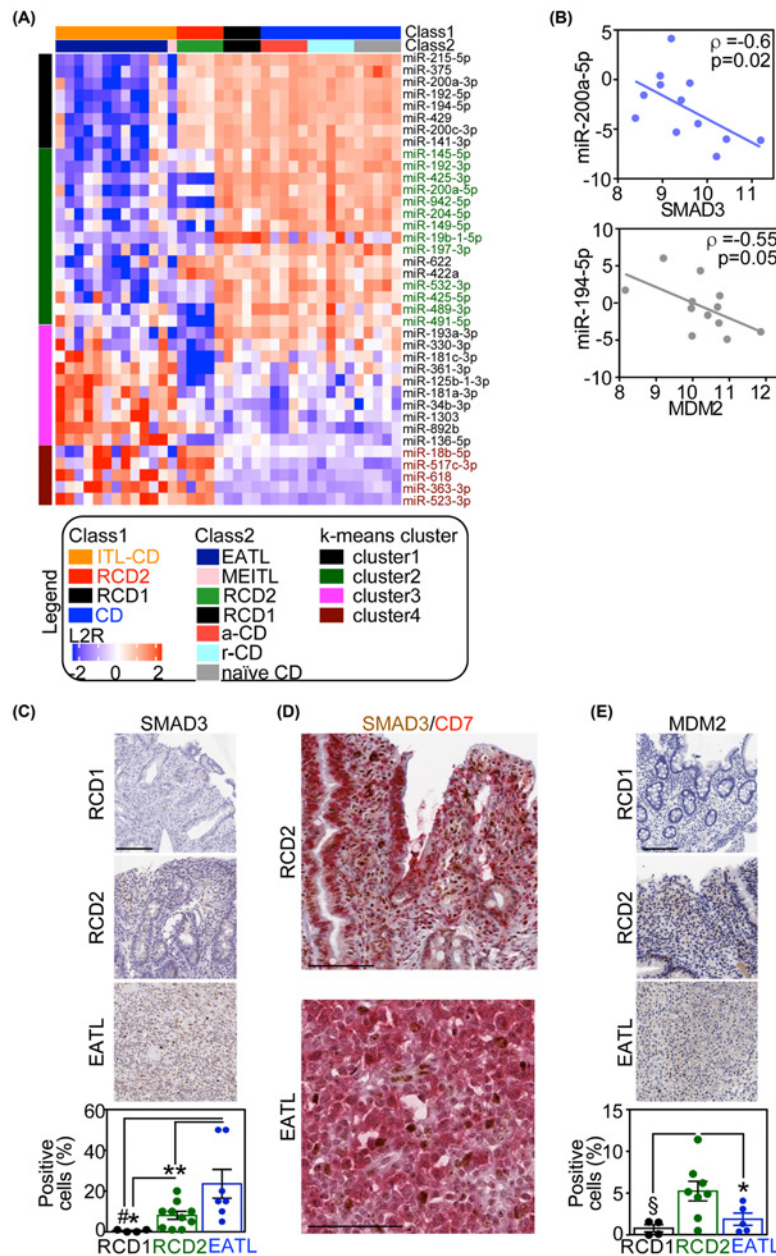


Figure 4. Progressive miR-200 and miR-192/215 miRNAs decrease with SMAD3 and MDM2 up-regulation characterizes RCD2 and ITL

(A) Heatmap of the RF-signature of 38 miRNAs in patients with previous or current history of CD with ITL, RCD1, RCD2 or different stages of CD. K-means clustering analysis was performed to identify groups of co-regulated miRNAs. a-CD, active CD despite GFD; r-CD, CD in remission after GFD. (B) Predicted protein targets of k-means cluster 2 miRNAs (identified using miRTargetLink Human algorithm; Supplementary Table S7) and their associated signaling were visualized and analyzed using STRING database. The top predicted pathways (from KEGG) specific to k-means cluster 2 miRNAs are also indicated (Supplementary Table S9 for the complete list). (C) Inverse correlation between the indicated miRNA and the predicted target was performed in ITL-CD for which both expression data were available ($n=12$). ρ , Spearman's coefficient of rank correlation. (D) Nuclear localization and protein expression of SMAD3 was evaluated in a second series of RCD1, RCD2 and EATL cases (Supplementary Table S1 for details) by IHC. Bottom, quantification of SMAD3-positive cells. *, $P=0.03$; **, $P=0.009$; #, $P=0.003$ by Mann-Whitney's U test. Scale bar, 100 μm . (E) Double IHC for SMAD3 (marked in brown) and CD7 (marked in red) in representative RCD2 and EATL cases showing co-expression of the two markers. Scale bars, 100 μm . (F) Nuclear localization and protein expression of MDM2 was evaluated in the second series of RCD1, RCD2 and EATL cases (see Supplementary Table S1 for details) by IHC. Bottom, quantification of MDM2-positive cells. §, $P=0.01$; *, $P=0.04$ by Mann-Whitney's U test. Scale bar, 100 μm .

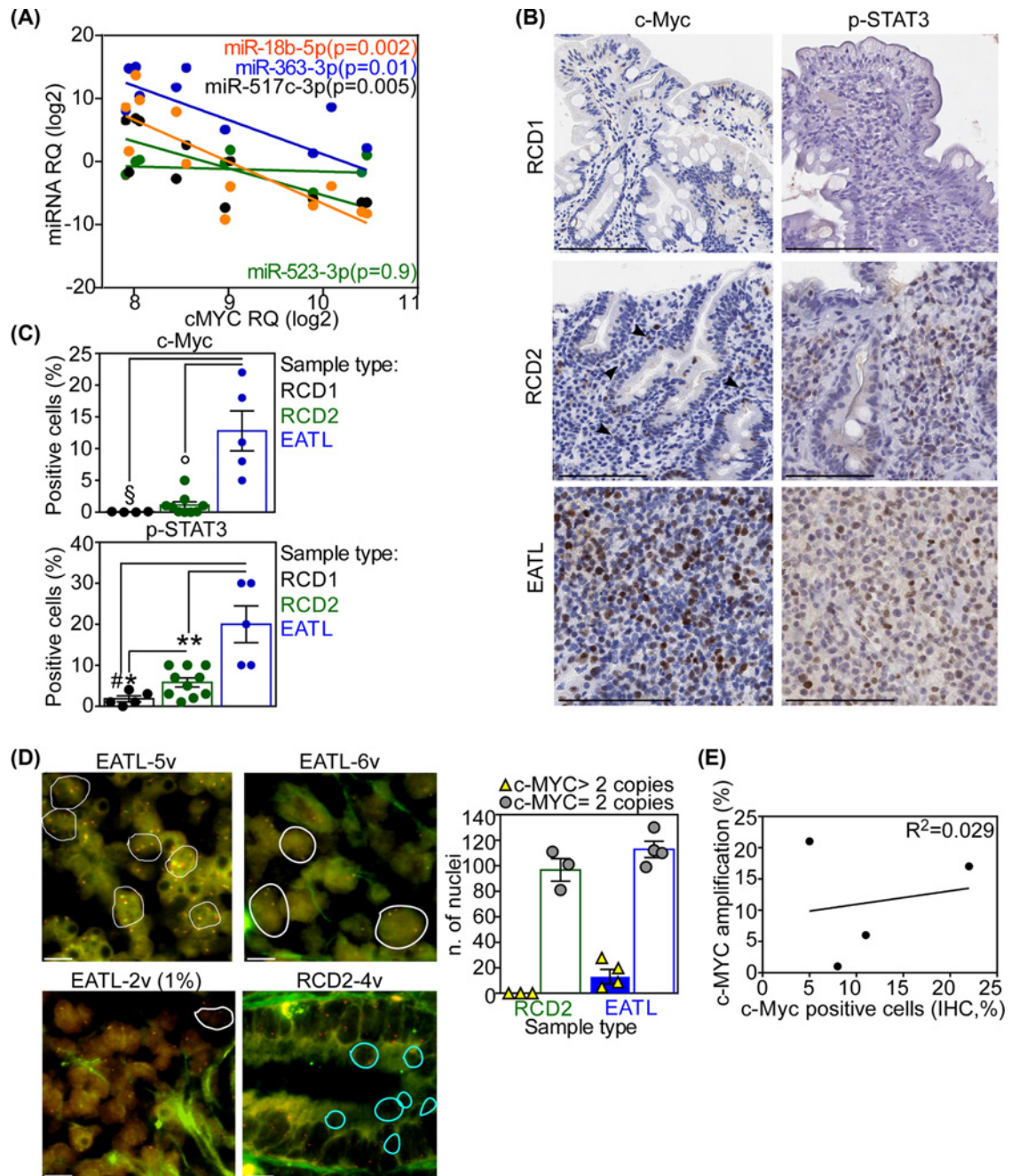


Figure 5. Up-regulation of C19MC and miR-17/92 miRNAs in RCD2 and ITL with CD correlates with c-MYC/STAT3 signaling activity

(A) Inverse correlation between the indicated miRNAs and cMYC mRNA was performed in and ITL with CD for which both expression data were available ($n=12$). The Spearman's rank correlation coefficients are: $\rho = -0.79$ (miR-18b-5p), $\rho = -0.67$ (miR-363-3p), $\rho = -0.75$ (miR-517c-3p) and $\rho = 0.07$ (miR-523-3p). (B, C) Nuclear localization and protein expression of c-MYC and phosphorylated STAT3 at Tyr⁷⁰⁵ (pSTAT3) was evaluated in the second series of RCD1, RCD2 and EATL cases (Supplementary Table S1 for details) by IHC and the percentage of positive cells was quantified (C). Scale bars, 100 μm . §, $P=0.001$; °, $P=0.016$; #, $P=0.005$; *, $P=0.03$; **, $P=0.008$ by Mann-Whitney's U test. (D) c-MYC analysis by FISH (overlay) with a dual color break apart probe is shown for representative EATL and RCD cases. Nuclei with gene amplification are circled in white, while blue circles indicate IEL present within RCD2 mucosa. Single-color pictures are provided in Supplementary Figure S5B,C. Scale bar, 10 μm . Right, quantification in the indicated sample type of nuclei with normal (i.e. =2) or amplified (>2 copies per nuclei) c-MYC. (E) Correlation between c-Myc amplification (percentage of positive nuclei from FISH analysis) and protein expression (percentage of positive nuclei from IHC staining) was evaluated in each EATL case ($n=4$). ITL-CD, ITL with CD.

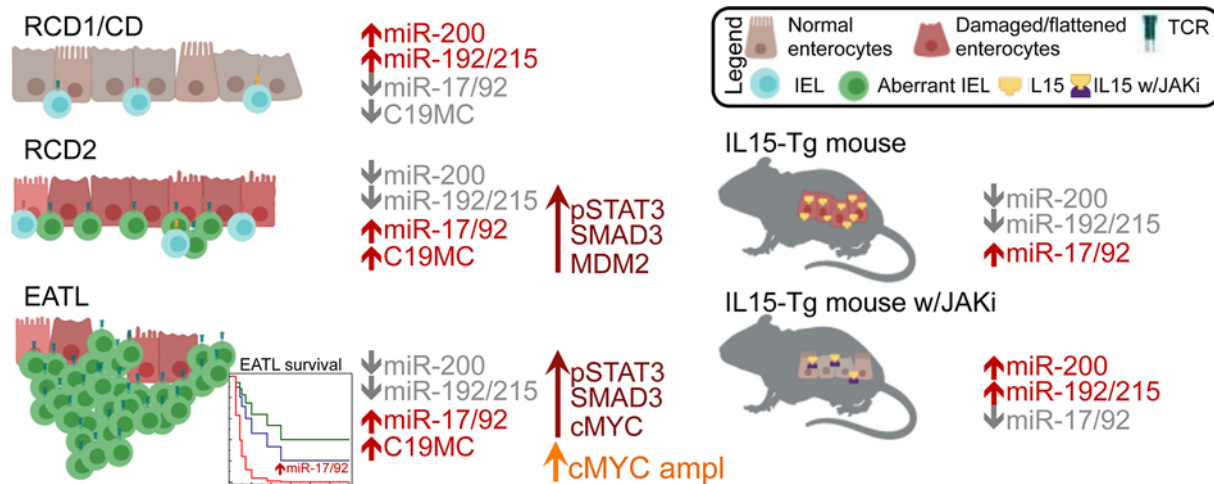


Figure 6. Schematic of the proposed model

Discussion

In the present study, we provide initial characterization of miRNAs and associated signaling pathways specific to ITLs and refractory type-2 CD, a preneoplastic condition that affects approximately 5–10% of all CD patients. We have identified that ITLs have a specific miRNA signature centered on overexpression of the chromosome 19 miRNA cluster C19MC with respect to other PTCLs. We also found that another oncogenic miRNA cluster, the miR-17/92, is overexpressed in MEITL as compared with EATL, and in EATL patients with poorer prognosis. Next, we have focused only on CD patients and searched for miRNAs potentially able to discriminate among CD, RCD and intestinal lymphoma (ITL-CD) diseases. Our data propose that a coordinated repression of oncosuppressive miR-200 and miR-192/215 coupled with the overexpression of the two oncogenic miRNA clusters C19MC and miR-17/92 might promote and sustain the neoplastic transformation of the aberrant intraepithelial T-cell clone in RCD2 patients. At the protein level this is accompanied by increased nuclear SMAD3 and MDM2 expression, which is paralleled by STAT3 activation and eventually results in c-Myc overexpression into full-blown lymphoma. To better understand if these miRNAs could have a pathogenic role in intestinal lymphomagenesis, we analyzed their expression in the IL-15 TG mouse model either left untreated or after treatment with the pan-JAKi Tofacitinib. This mouse model recapitulates, at least in part, the inflammatory state characteristic of human RCD. The IL-15 TG mice do not display gluten sensitivity, yet they strikingly recapitulate many of the intestinal pathologic features seen in CD patients. The IL-15 transgene in these mice are expressed from a mouse enterocyte specific T3^b promoter that is active throughout the small intestines, yet the inflammatory pathologic lesions are anatomically confined to the duodeno-jejunal region of the small intestines. Furthermore, as seen in CD patients, in addition to the extensive localized blunting and atrophy of intestinal villi in the proximal small intestines, there is marked accumulation of plasma cells in the underlying lamina propria along with hypergammaglobulinemia and the presence of autoantibodies against tissue-transglutaminase 2 thus collectively representing some of both T- and B-cell-mediated effects seen in CD. The treatment of these mice with tofacitinib, a pan JAKi that abrogates IL-15 signaling, results in the complete reversal of pathologic manifestations in the proximal small intestines [6].

In support of our findings, the miR-200 and miR-192/215 levels were decreased while miR-17/92 miRNAs were up-regulated in the mice small bowel. Further, JAK inhibition partly reverted the expression of RCD2-dysregulated miRNAs. Interestingly Tofacitinib is already used in other inflammatory diseases [3] including ulcerative colitis and Chron's disease [23] and could represent a novel therapeutic for RCD2. Lastly, the similarity analysis of the samples based on the identified miRNA signature revealed that RCD2 are more close to RCD1 than to lymphomas. This supports the concept that RCD2 are not yet full-blown lymphomas and suggest that target treatments, such as IL15/STAT3/JAK blocking, might revert RCD2 to less severe RCD1 or CD stages.

All these miRNAs have been previously documented as crucial players in tumorigenesis and matrix remodeling [24,25] and a role for miR-192/215 family in CD has been previously described [7,26]. Furthermore, the analysis of co-upregulated miRNAs in RCD2 and ITL-CD indicated once again a role for C19MC and miR-17/92 miRNAs in sustaining the tumorigenesis of aberrant T cells in CD. Both miRNA families are known to be part of an oncogenic feedback loop with MYC [20,27]. In line with this, analysis of nuclear expression of c-Myc or its upstream regulator

STAT3 [21,22] in RCD1, RCD2 and EATL specimens has showed that activated STAT3 is a feature shared by RCD2 and EATL cases, whereas c-Myc is mainly overexpressed in lymphomas where it is also amplified in a portion of neoplastic cells. Interestingly, JAK1 or STAT3 activating mutations have been previously described in RCD2 as major drivers of intraepithelial lymphocytes neoplastic transformation [28]. Moreover, pro-tumorigenic circuits between miRNAs and c-Myc has been described in solid tumors and in lymphomas [29] as well as at different stages of tumor initiation and progression [27].

Although CD rarely evolves into RCD, the incidence of subjects with CD is increasing worldwide. GFD is the only approach to control CD and RCD2 patients are usually treated with the general chemotherapeutic/immunosuppressant cladribine, [1] or with autologous hemopoietic stem cell transplantation [3]. However a rationale to guide a personalized approach for patients' management or treatment does not exist to date.

In this scenario the identification of novel biomarkers to guide patients' stratification into risk categories is urgently needed in order to transform the general approach to CD patients' management into a personalized one. Despite our results provide a preliminary overview of deregulated miRNAs/targets circuits, they collectively represent an initial step in the understanding of molecular pathogenesis of RCD2 and related EATL and potentially contribute in designing a personalized therapeutic approach for these diseases.

Clinical perspectives

- RCD2 and EATL are rare but deadly complications of CD. Although initial knowledge of intraepithelial T-cells transformation has been acquired, the molecular determinants that contribute to these diseases remain poorly defined.
- Here we show that deregulation of the c-MYC-related miRNA cluster miR17/92 and of miR-200 and miR-192/215 families occurs in the transition from indolent CD to RCD2 and EATL. The miRNAs targeting SMAD3, MDM2 and activated STAT3 are more expressed in RCD2 and EATL with respect to RCD1 whereas c-Myc is expressed mostly by EATL. In the TG mouse model of RCD2, these miRNAs are perturbed and treatment with a JAKi partially reverts miRNAs-targetderegulation in mice intestine.
- Our results provide novel insights into miRNAs-target proteins circuits involved in the neoplastic transformation of aberrant intraepithelial T cells and provide preliminary evidence about molecular mechanism of JAKi in RCD2.

Competing Interests

The authors declare that there are no competing interests associated with the manuscript.

Funding

This work was supported by the Italian Minister of Health [grant numbers GR2011-02351626 (to V.V.), GR2011-02348234 (to L.E.)]; and the AIRC 5x1000 [grant number 21198 (to S.P)].

Author Contribution

V.V., L.E., S.P. and S.B. were responsible for study concept and design. V.V., G.G., M.A.L., S.F. and S.F. performed the experiments. V.V., G.G., C.A. and A.T. were responsible for analysis and interpretation of data. S.B. and S.P. were responsible for study supervision. A.T. was responsible for statistical analyses. L.R., V.L., A.V., A.D.S., M.V., L.P.P., C.A., M.P. and S.P. were responsible for acquisition of data and technical or material support. V.V. and L.E. drafted the manuscript. S.B., S.P. and L.E. obtained funding. All authors critically revised and approved the manuscript for important intellectual content.

Abbreviations

AITL, angioimmunoblastic T-cell lymphoma; ALK, Anaplastic lymphoma kinase; CD, celiac disease; DAB, 3'-Diaminobenzidine; EATL, enteropathy-associated T-cell lymphoma; EBV, Epstein-Barr virus; ENKL, extranodal nasal-type NK/T-cell lymphoma; FFPE, formalin-fixed paraffin-embedded; FISH, fluorescence *in situ* hybridization; GFD, gluten-free diet; IHC, immunohistochemistry; IL15, interleukin-15; ITL, intestinal T-cell lymphoma; JAK, Janus kinase; JAKi, JAK inhibitor; MDM2, Mouse double

minute 2 homolog; MEITL, monomorphic epitheliotropic intestinal T-cell lymphoma; miRNA, microRNA; NMF, non-negative matrix factorization; NOS, not otherwise specified; ncRNA, non-coding RNA; PCA, principal component analysis; PTCL, peripheral T-cell lymphoma; RCD, refractory celiac disease; SMAD3, Mothers Against Decapentaplegic Homolog 3; TCR, T-cell receptor; TG, transgenic.

References

- 1 Rubio-Tapia, A. and Murray, J.A. (2010) Classification and management of refractory coeliac disease. *Gut* **59**, 547–557, <https://doi.org/10.1136/gut.2009.195131>
- 2 Cellier, C., Patey, N., Mauvieux, L. et al. (1998) Abnormal intestinal intraepithelial lymphocytes in refractory sprue. *Gastroenterology* **114**, 471–481, [https://doi.org/10.1016/S0016-5085\(98\)70530-X](https://doi.org/10.1016/S0016-5085(98)70530-X)
- 3 Woodward, J. (2016) Improving outcomes of refractory celiac disease - current and emerging treatment strategies. *Clin. Exp. Gastroenterol* **9**, 225–236, <https://doi.org/10.2147/CEG.S87200>
- 4 Abadie, V. and Jabri, B. (2014) IL-15: a central regulator of celiac disease immunopathology. *Immunol. Rev.* **260**, 221–234, <https://doi.org/10.1111/imr.12191>
- 5 Yokoyama, S., Watanabe, N., Sato, N. et al. (2009) Antibody-mediated blockade of IL-15 reverses the autoimmune intestinal damage in transgenic mice that overexpress IL-15 in enterocytes. *Proc. Natl. Acad. Sci. U.S.A.* **106**, 15849–15854, <https://doi.org/10.1073/pnas.0908834106>
- 6 Yokoyama, S., Perera, P.-Y., Waldmann, T.A., Hiroi, T. and Perera, L.P. (2013) Tofacitinib, a Janus kinase inhibitor demonstrates efficacy in an IL-15 transgenic mouse model that recapitulates pathologic manifestations of celiac disease. *J. Clin. Immunol.* **33**, 586–594, <https://doi.org/10.1007/s10875-012-9849-y>
- 7 Vaira, V., Roncoroni, L., Barisani, D. et al. (2014) microRNA profiles in coeliac patients distinguish different clinical phenotypes and are modulated by gliadin peptides in primary duodenal fibroblasts. *Clin. Sci.* **126**, <https://doi.org/10.1042/CS20130248>
- 8 Laginestra, M.A., Piccaluga, P.P., Fuligni, F. et al. (2014) Pathogenetic and diagnostic significance of microRNA deregulation in peripheral T-cell lymphoma not otherwise specified. *Blood Cancer J.* **4**, e259, <https://doi.org/10.1038/bcj.2014.78>
- 9 Swerdlow, S.H. and World Health Organization (2019) International Agency for Research on Cancer. *WHO Classification of Tumours of Haematopoietic and Lymphoid Tissues*, <http://publications.iarc.fr/Book-And-Report-Series/Who-larc-Classification-Of-Tumours/Who-Classification-Of-Tumours-Of-Haematopoietic-And-Lymphoid-Tissues-2017>
- 10 Ludvigsson, J.F., Leffler, D.A., Bai, J.C. et al. (2013) The Oslo definitions for coeliac disease and related terms. *Gut* **62**, 43–52, <https://doi.org/10.1136/gutjnl-2011-301346>
- 11 Al-Toma, A., Volta, U., Auricchio, R. et al. (2019) European Society for the Study of Coeliac Disease (ESsCD) guideline for coeliac disease and other gluten-related disorders. *United Eur. Gastroenterol. J.* **7**, 583–613, <https://doi.org/10.1177/2050640619844125>
- 12 Augello, C., Gianelli, U., Savi, F. et al. (2014) MicroRNA as potential biomarker in HCV-associated diffuse large B-cell lymphoma. *J. Clin. Pathol.* **67**, 697–701, <https://doi.org/10.1136/jclinpath-2014-202352>
- 13 Du, P., Kibbe, W.A. and Lin, S.M. (2008) lumi: a pipeline for processing Illumina microarray. *Bioinformatics* **24**, 1547–1548, <https://doi.org/10.1093/bioinformatics/btn224>
- 14 Augello, C., Colombo, F., Terrasi, A. et al. (2018) Expression of C19MC miRNAs in HCC associates with stem-cell features and the cancer-testis genes signature. *Dig. Liver Dis.* **50**, 583–593, <https://doi.org/10.1016/j.dld.2018.03.026>
- 15 Terrasi, A., Bertolini, I., Martelli, C. et al. (2019) Specific V-ATPase expression sub-classifies IDHwt lower-grade gliomas and impacts glioma growth *in vivo*. *EBioMedicine* **41**, 214–224, <https://doi.org/10.1016/j.ebiom.2019.01.052>
- 16 Díaz-Urriarte, R. and Alvarez de Andrés, S. (2006) Gene selection and classification of microarray data using random forest. *BMC Bioinformatics* **7**, 3, <https://doi.org/10.1186/1471-2105-7-3>
- 17 Szklarczyk, D., Gable, A.L., Lyon, D. et al. (2019) STRING v11: protein–protein association networks with increased coverage, supporting functional discovery in genome-wide experimental datasets. *Nucleic Acids Res.* **47**, D607–D613, <https://doi.org/10.1093/nar/gky1131>
- 18 Mogilyansky, E. and Rigoutsos, I. (2013) The miR-17/92 cluster: a comprehensive update on its genomics, genetics, functions and increasingly important and numerous roles in health and disease. *Cell Death Differ.* **20**, 1603–1614, <https://doi.org/10.1038/cdd.2013.125>
- 19 Dal Bo, M., Bomben, R., Hernández, L. and Gattei, V. (2015) The MYC/miR-17-92 axis in lymphoproliferative disorders: A common pathway with therapeutic potential. *Oncotarget* **6**, 19381–19392, <https://doi.org/10.18632/oncotarget.4574>
- 20 Sin-Chan, P., Mumal, I., Suwal, T. et al. (2019) A C19MC-LIN28A-MYC oncogenic circuit driven by hijacked super-enhancers is a distinct therapeutic vulnerability in ETMRs: a lethal brain tumor. *Cancer Cell* **36**, 51–67.e7, <https://doi.org/10.1016/j.ccell.2019.06.002>
- 21 Bowman, T., Broome, M.A., Sinibaldi, D. et al. (2001) Stat3-mediated Myc expression is required for Src transformation and PDGF-induced mitogenesis. *Proc. Natl. Acad. Sci. U.S.A.* **98**, 7319–7324, <https://doi.org/10.1073/pnas.131568898>
- 22 Demaria, M., Misale, S., Giorgi, C. et al. (2012) STAT3 can serve as a hit in the process of malignant transformation of primary cells. *Cell Death Differ.* **19**, 1390–1397, <https://doi.org/10.1038/cdd.2012.20>
- 23 Weisshof, R., Golan, M.A., Yvellez, O.V. and Rubin, D.T. (2018) The use of tofacitinib in the treatment of inflammatory bowel disease. *Immunotherapy* **10**, 837–849, <https://doi.org/10.2217/imt-2018-0015>
- 24 Feng, X., Wang, Z., Fillmore, R. and Xi, Y. (2014) MIR-200, a new star miRNA in human cancer. *Cancer Lett.* **344**, 166–173, <https://doi.org/10.1016/j.canlet.2013.11.004>
- 25 Hong, J.P., Li, X.M. and Zheng, F.L. (2013) VEGF suppresses epithelial-mesenchymal transition by inhibiting the expression of Smad3 and miR-192, a Smad3-dependent microRNA. *Int. J. Mol. Med.* **31**, 1436–1442, <https://doi.org/10.3892/ijmm.2013.1337>

- 26 Magni, S., Buoli Comani, G., Elli, L. et al. (2014) miRNAs affect the expression of innate and adaptive immunity proteins in celiac disease. *Am. J. Gastroenterol.* **109**, 1662–1674, <https://doi.org/10.1038/ajg.2014.203>
- 27 Mihailovich, M., Bremang, M., Spadotto, V. et al. (2015) miR-17-92 fine-tunes MYC expression and function to ensure optimal B cell lymphoma growth. *Nat. Commun.* **6**, 8725, <https://doi.org/10.1038/ncomms9725>
- 28 Ettersperger, J., Montcuquet, N., Malamut, G. et al. (2016) Interleukin-15-dependent T-cell-like innate intraepithelial lymphocytes develop in the intestine and transform into lymphomas in celiac disease. *Immunity* **45**, 610–625, <https://doi.org/10.1016/j.immuni.2016.07.018>
- 29 Psathas, J.N. and Thomas-Tikhonenko, A. (2014) MYC and the art of microRNA maintenance. *Cold Spring Harb. Perspect. Med.* **4**, a014175, <https://doi.org/10.1101/cshperspect.a014175>